Chemical Science

ROYAL SOCIETY OF CHEMISTRY

EDGE ARTICLE

View Article Online
View Journal | View Issue

Check for updates

Cite this: *Chem. Sci.*, 2020, **11**, 5766

All publication charges for this article have been paid for by the Royal Society of Chemistry

Facile benzene reduction promoted by a synergistically coupled Cu–Co–Ce ternary mixed oxide†

Hao Chen,‡[ab] Wenwen Lin,‡[a] Zihao Zhang,‡[a] Zhenzhen Yang,[b] Kecheng Jie,[b] Jie Fu,*[a] Shi-ze Yang*[d] and Sheng Dai*[bc]

Received 20th April 2020
Accepted 14th May 2020

DOI: 10.1039/d0sc02238a

rsc.li/chemical-science

Hydrogenation of aromatic rings promoted by earth-abundant metal composites under mild conditions is an attractive and challenging subject in the long term. In this work, a simple active site creation and stabilization strategy was employed to obtain a Cu^+-containing ternary mixed oxide catalyst. Simply by pre-treatment of the ternary metal oxide precursor under a H_2 atmosphere, a Cu^+-derived heterogeneous catalyst was obtained and denoted as $Cu_1Co_5Ce_5O_x$. The catalyst showed (1) high Cu^+ species content, (2) a uniform distribution of Cu^+ doped into the lattices of CoO_x and CeO_2, (3) formation of CoO_x/CuO_x and CeO_2/CuO_x interfaces, and (4) a mesoporous structure. These unique properties of $Cu_1Co_5Ce_5O_x$ endow it with pretty high hydrogenation activity for aromatic rings under mild conditions (100 °C with 5 bar H_2), which is much higher than that of the corresponding binary counterparts and even exceeds the performance of commercial noble metal catalysts (*e.g.* Pd/C). The synergetic effect plays a crucial role in the catalytic procedure with CeO_2 functioning as a hydrogen dissociation and transfer medium, Cu^+ hydrogenating the benzene ring and CoO_x stabilizing the unstable Cu^+ species. This will unlock a new opportunity to design highly efficient earth-abundant metal-derived heterogeneous catalysts *via* interface interactions.

Open Access Article. Published on 22 May 2020. Downloaded on 2/9/2026 12:03:23 AM.
This article is licensed under a Creative Commons Attribution-NonCommercial 3.0 Unported Licence.

Hydrogenation is one of the central themes of petrochemical, coal chemical, fine chemical and environmental industries and is one of the most intensively investigated topics in catalysis.[1–4] In addition, in the synthesis of fine chemicals, reduction of various functional groups, such as –C=C, –C≡C, –C=O, $–NO_2$, –C≡N, –COOH, and $–CONH_2$, is required to afford the corresponding alkanes, alkenes, alcohols, and amine products that are key intermediates for the fine chemical, polymer, agrochemical, and pharmaceutical industries, especially using H_2 as a clean and cheap hydrogen source.[5,6] Among all these transformations, hydrogenation of benzene is a direct and important approach to afford cycloalkane intermediates for petrochemical and agrochemical production, and has received enormous attention over the past few decades.[7–9] However, the π-conjugation in aromatic rings makes it one of the most robust chemical bonds due to high aromaticity and non-polarity.[10–12] Over the past few decades, technologies mainly depending on expensive and precious metal-based catalysts, such as Pd, Ru, Pt, and Ir, have been extensively investigated to facilitate this transformation. Concerns over the scarcity and high cost of noble metals have driven the search for nonprecious earth-abundant alternatives with comparable activity, selectivity and stability, which are greatly desired for scalable and cost-effective chemical transformations.[11–18] To date, there have been a few reports on Ni/Al_2O_3, Ni/SiO_2, Co/SiO_2 and Ni–Al alloys that can partially or fully hydrogenate benzene with transition metal-based catalysts, but harsh reaction conditions (*e.g.* high reaction temperature up to 200 °C and high H_2 pressure up to 8 MPa) and low weight hourly space velocity (WHSV) limit their further application.[19–21] Therefore, despite intensive studies on the subject of benzene hydrogenation, catalytic systems based on nonprecious metals capable of promoting the reaction under mild conditions are still rarely reported. There are still significant challenges in developing cheap, easily synthesized and highly efficient heterogeneous catalysts derived from earth-abundant alternatives by rational design.

From this aspect, we focus our attention on one of the most challenging kinds of metal species based on copper, which is pretty cheap and abundant. On the other hand, copper-based catalysts have been widely investigated for the hydrogenation

[a]*Key Laboratory of Biomass Chemical Engineering of Ministry of Education, College of Chemical and Biological Engineering, Zhejiang University, Hangzhou 310027, China. E-mail: jiefu@zju.edu.cn*

[b]*Department of Chemistry, University of Tennessee, Knoxville, TN 37996, USA*

[c]*Chemical Sciences Division, Oak Ridge National Laboratory, Oak Ridge, TN 37831, USA. E-mail: dais@ornl.gov*

[d]*Eyring Materials Center, Arizona State University, Tempe, 85257, USA. E-mail: shize.yang@asu.edu*

† Electronic supplementary information (ESI) available. See DOI: 10.1039/d0sc02238a

‡ These authors contributed equally.

This journal is © The Royal Society of Chemistry 2020

Open Access Article. Published on 22 May 2020. Downloaded on 2/9/2026 12:03:23 AM.
This article is licensed under a Creative Commons Attribution-NonCommercial 3.0 Unported Licence.

of biomass[22,23] and CO_2,[24–27] with the activity being mainly attributed to the Cu^0 species in vapor-phase reactions.[23,28] For instance, Ma *et al.* revealed that the formation rate of alcohol is strongly correlated with the density of surface Cu^0 sites.[25,29] Notably, compared with Cu^0 and Cu^{2+}, Cu^+ has a higher hydrogenation activity considering its intrinsic ability to facilitate electron transfer through gaining or losing an electron.[25,30,31] Many studies have reported that Cu^0/Cu^+ leads to an enhanced catalytic activity for hydrogenation, which is attributed to the activation of the ester groups by Cu^+ species in the production of alcohols.[30,32–34] However, these conjectures are inconclusive as obtaining Cu^+ is synthetically challenging due to its tendency to easily oxidize to Cu^{2+} or reduce to Cu^0 during catalyst preparation and processing. The key to success lies in the design and fabrication of copper-containing composites capable of stabilizing the highly active Cu^+ species through interface interactions. This will also enable a deeper understanding of the catalytic contributions from the Cu^+ species, which is significant for the rational design of active hydrogenation catalysts.

As previously reported, the CoO_y in Cu catalyst not only enhances the metallic Cu dispersion and H_2 activation ability, but also modifies the chemical states of Cu to create suitable surface Cu^0/Cu^+ distributions due to strong electronic interactions at the Cu/CoO_x interface.[35] This inspires us to fabricate multi-component heterogeneous catalysts containing Cu^+ species. It is known that the adsorption and activation of H_2 constitutes another critical step in the hydrogenation reactions. Various kinds of materials have been reported to activate H_2 by homolytic or heterolytic dissociation.[36,37] Recently, Sai *et al.* created solid frustrated Lewis pairs (FLPs) on the surface of CeO_2 by regulating their surface defects. The resultant catalysts exhibited H_2 dissociation ability with a low activation barrier and delivered a high catalytic activity for hydrogenation of alkenes and alkynes, as well as transformation of CO_2.[38,39] However, the catalytic activity of these CeO_2-based materials is still insufficient to achieve hydrogenation of aromatic rings. Therefore, we expect that the combination of Cu, Co and Ce species will create enhanced H_2 activation capability, realize the hydrogenation of aromatic rings under mild conditions through a synergistic effect, and lead to further understanding of the interface interaction during the catalytic procedure.

In previous studies, our group developed a simple fabrication procedure to obtain a ternary $CuO–Co_3O_4–CeO_2$ catalyst, which showed excellent catalytic activity for CO oxidation.[40] Herein, a simple active site creation and stabilization strategy was employed to obtain a Cu^+-containing ternary mixed oxide catalyst. Simply by pre-treatment of the ternary metal oxide precursor under a H_2 atmosphere, a Cu^+-derived heterogeneous catalyst was obtained and denoted as $Cu_1Co_5Ce_5O_x$. The catalyst showed (1) high Cu^+ species content, (2) a uniform distribution of Cu^+ doped into the lattices of CoO_x and CeO_2, (3) formation of CoO_y/CuO_x and CeO_2/CuO_x interfaces, and (4) a mesoporous structure. These unique properties of $Cu_1Co_5Ce_5O_x$ endow it with pretty high hydrogenation activity for aromatic rings under mild conditions (100 °C with 5 bar H_2), which is much higher than that of the corresponding binary counterparts and even exceeds the performance of commercial noble metal catalysts (*e.g.* Pd/C). The synergetic effect plays a crucial role in the catalytic procedure with CeO_2 functioning as a hydrogen dissociation and transfer medium, Cu^+ hydrogenating the benzene ring and CoO_x stabilizing the unstable Cu^+ species. This will unlock a new opportunity to design highly efficient earth-abundant metal-derived heterogeneous catalysts *via* interface interactions.

The ternary $Cu_1Co_5Ce_5O_x$ catalyst was prepared *via* a two-step approach involving co-precipitation and heat-treatment. $Cu_1Co_5Ce_5O_y$ with a Cu : Co : Ce atomic ratio of 1 : 5 : 5 was first synthesized using a co-precipitation method,[40,41] and further pre-treatment at 100 °C with 5 bar H_2 for 24 h leads to the formation of $Cu_1Co_5Ce_5O_x$. The ICP result shown in Table S1† confirmed that the Cu : Co : Ce atomic ratio was almost the same as that calculated from the raw ratio. The XRD pattern of $Cu_1Co_5Ce_5O_y$ in Fig. 1a suggests that the as-synthesized ternary oxides are composed of crystalline CeO_2 and Co_3O_4. After H_2 heat-treatment, no change in the diffraction peaks of CeO_2 and Co_3O_4 was found in $Cu_1Co_5Ce_5O_x$. Then, we compared the XRD pattern of CeO_2 (PDF#81-0792),[42] Co_3O_4 (PDF-74-1657)[43] and $Cu_1Co_5Ce_5O_x$ as shown in Fig. 1(a) to further prove that Cu is doped into the lattices of CoO_y and CeO_2 in $Cu_1Co_5Ce_5O_x$. It was found that the XRD peaks for Ce and Co in $Cu_1Co_5Ce_5O_x$ shifted to lower 2 theta angle, which means a larger lattice parameter of the CeO_2 and Co_3O_4 in $Cu_1Co_5Ce_5O_x$ than the pure CeO_2 and Co_3O_4 after the introduction of copper species, as well as providing evidence to show that the Cu ions are incorporated into the CeO_2 and Co_3O_4 crystallites in $Cu_1Co_5Ce_5O_x$.[42,44] Then we investigated the structure of $CuCoO_x$ (Cu : Co = 1 : 10 mole ratio), $CuCeO_x$ (Cu : Ce = 1 : 10 mole ratio) and $CoCeO_x$ (Ce : Co = 1 : 1 mole ratio) by XRD and the results are shown in Fig. S1.† The results showed that the 10 mol% Cu dispersed well in the CoO_x and CeO_x with almost no Cu XRD peak observed. Thus, in this work, the Cu uniformly distributed among CoO_y and CeO_2, respectively. XPS was performed to probe the oxidation states of Co and Cu on the surface of the ternary oxides. As shown in Fig. 1b–d, both Cu 2p and Co 2p peaks exhibit peak shifts towards lower energies, indicating that the H_2 pre-treatment significantly reduces the surface of $Cu_1Co_5Ce_5O_y$ and partially lowers the oxidation states of the metal species (Cu^{2+} 934.1 eV, Co^{3+} 781.2 eV, Cu^+/Cu^0 932.0 eV and Co^{2+} 779.2 eV, Table S2†).[45] Considering the overlap of the XPS peaks corresponding to Cu^+ and Cu^0, we turned to Cu LMM to determine the Cu oxidation states in the ternary oxide catalysts (Fig. 1d and S2†), where only Cu^{2+} (569.3 eV) was observed in the $Cu_1Co_5Ce_5O_y$ catalyst while only Cu^+ (573.2 eV) was observed in the $Cu_1Co_5Ce_5O_x$ catalyst.[46–48] Therefore, the spectroscopic results indicate that Cu^+ and Co^{2+} are formed on the surface of $Cu_1Co_5Ce_5O_x$ after the H_2 pre-treatment. CeO_2 exhibits hydrogenation activity for unsaturated compounds as the oxidation states of Ce can change reversibly between Ce^{4+} under oxidizing conditions and Ce^{3+} under reducing conditions.[49,50] As shown in Fig. 1e, XPS has been performed for $Cu_1Co_5Ce_5O_y$ and $Cu_1Co_5Ce_5O_x$ to distinguish between the Ce^{4+} and Ce^{3+} species, where the shifting of peaks to lower

Open Access Article. Published on 22 May 2020. Downloaded on 2/9/2026 12:03:23 AM.
This article is licensed under a Creative Commons Attribution-NonCommercial 3.0 Unported Licence.

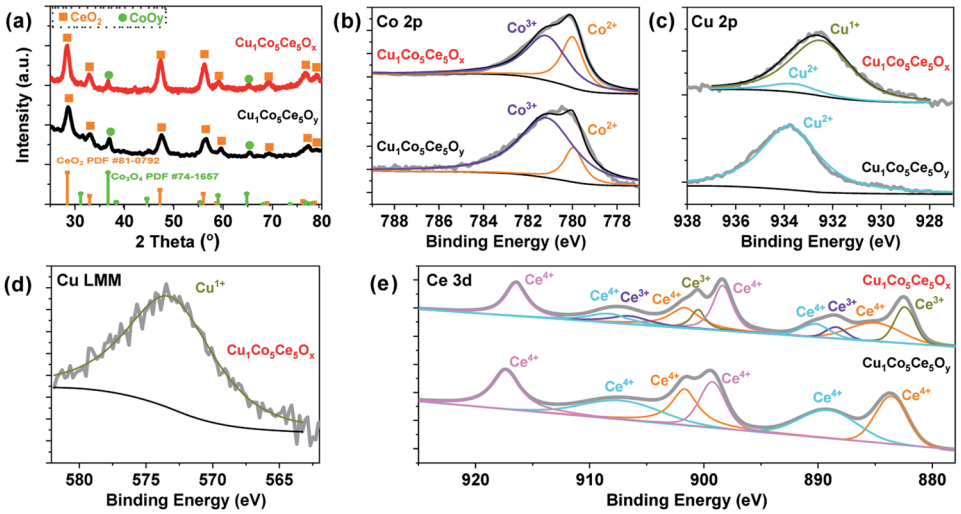

Fig. 1 (a) XRD patterns, and (b) XPS results of Co 2p, (c) Cu 2p, (d) Cu-LMM, and (e) Ce 3d in $Cu_1Co_5Ce_5O_y$ and $Cu_1Co_5Ce_5O_x$ obtained before and after pre-treatment under 5 bar H_2 and 100 °C temperature for 24 h.

binding energy may be due to a higher proportion of Ce^{3+}.[50] Chen *et al.*[51] reported that active Cu clusters consist of Cu^0 at the top layer and Cu^+ species at the Cu/CeO_2 interface due to electron depletion caused by the oxygen vacancies (O_v) in CeO_2. In our case, the H_2 pre-treatment may create more oxygen vacancies which stabilize Cu^+ through forming Cu^+–O_v–Ce^{3+} interfacial bonds. It was found that the Cu species in $CuCoCeO_y$ after pre-treatment for 6 h and 18 h were almost maintained at the Cu^{2+} state (Fig. S3†). However, it seemed that the Co was easily reduced and more Co^{2+} was formed compared with the $CuCoCeO_y$ after pre-treatment for 6 h and 18 h. And for Ce, the Ce in $CuCoCeO_y$ after pre-treatment for 6 h have no significant change compared with the starting material, with all the Ce species in the state of Ce^{4+}. After pre-treatment for 18 h, a small amount of Ce^{3+} formed.

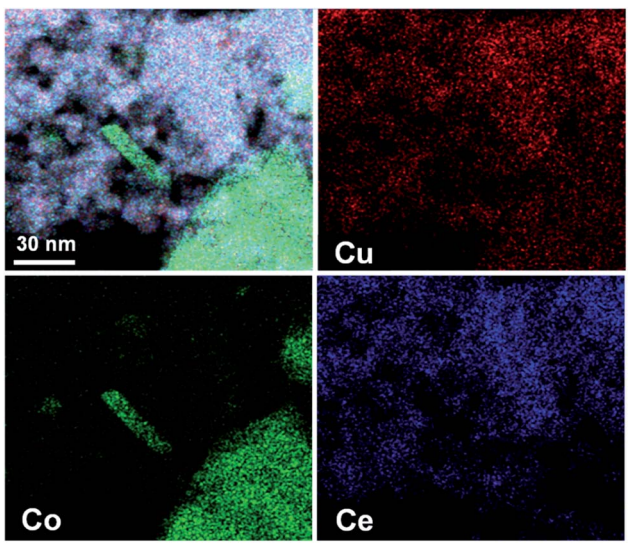

Fig. 2 STEM-HAADF images and EDS elemental mapping images of Cu, Co and Ce in the $Cu_1Co_5Ce_5O_x$ catalyst.

As reported in our previous work,[40,41] the as-synthesized $Cu_1Co_5Ce_5O_y$ without H_2 treatment showed a structure with copper–ceria and cobalt–ceria interfaces (Fig. S4†). To further probe the structural details of the ternary $Cu_1Co_5Ce_5O_x$ as well as the interface of $CoO_y(Cu_2O)$–$CeO_2(Cu_2O)$, STEM-HAADF with EDS elemental mapping was conducted as shown in Fig. 2. The absence of the diffraction peaks corresponding to Cu, Cu_2O, or CuO in the XRD pattern (Fig. 1a), together with a uniform distribution of Cu among CoO_y and CeO_2 in the STEM-EDS elemental maps (Fig. 2), suggests that Cu is doped into the lattices of CoO_y and CeO_2 for $Cu_1Co_5Ce_5O_x$ and forms CoO_y/CuO_x and CeO_2/CuO_x interfaces.

The N_2 adsorption–desorption isotherm at 77 K is shown in Fig. 3a and the sample exhibits a typical type IV shape isotherm, suggesting the existence of mesopores with 2–10 nm pore diameters in $Cu_1Co_5Ce_5O_x$ after H_2 treatment. The Brunauer–Emmett–Teller (BET) surface area of the $Cu_1Co_5Ce_5O_x$ is estimated to be 82 $m^2\ g^{-1}$ with a total pore volume of 0.13 $m^3\ g^{-1}$ (Fig. 3), which is a little higher compared with that of the $Cu_1Co_5Ce_5O_y$ before H_2 treatment (78 $m^2\ g^{-1}$). Notably, mesopores played a dominant role in the pore structure, contributing ~99% of the total pore volume (V_{micro} = 0 $m^3\ g^{-1}$, calculated using the *t*-plot method). For catalytic or adsorptive materials, a high surface area together with a mesoporous structure can dramatically enhance their reactivity due to an improved mass transfer effect.[52,53]

Acetyl benzene is selected as a model substrate to evaluate the catalytic properties of $Cu_1Co_5Ce_5O_x$ (Fig. 4a). In a typical catalytic experiment, 100 mg of $Cu_1Co_5Ce_5O_y$ was pre-treated at 100 °C with 5 bar H_2 for 24 h. Then 150 mg acetyl benzene (A) and 5 mL hexane were added to the reaction solution for hydrogenation under the same conditions. The H_2-pretreated ternary oxide catalyst $Cu_1Co_5Ce_5O_x$ exhibits excellent activity towards complete hydrogenation of both acetyl and benzene groups, producing ethylcyclohexane (D) with 100% conversion and 97% yield, which even exceeds the performance of

 This journal is © The Royal Society of Chemistry 2020

Open Access Article. Published on 22 May 2020. Downloaded on 2/9/2026 12:03:23 AM.
This article is licensed under a Creative Commons Attribution-NonCommercial 3.0 Unported Licence.

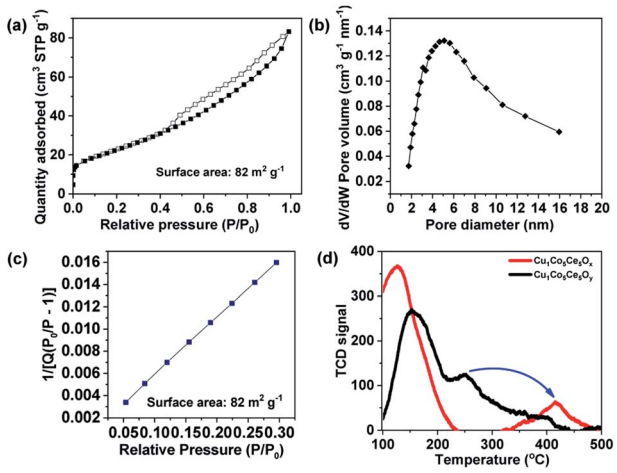

Fig. 3 (a) N_2 adsorption/desorption isotherm at 77 K, (b) pore size distribution curve, (c) BET plot, and (d) benzene temperature programmed desorption of $Cu_1Co_5Ce_5O_x$ and $Cu_1Co_5Ce_5O_y$ catalysts.

commercial 5 wt% Pd/C catalysts (74% conversion and 72% yield) under the same reaction conditions (Fig. 4b). Further control experiments show that the untreated ternary oxide catalyst $Cu_1Co_5Ce_5O_y$ exhibited much inferior hydrogenation capability, with ethylbenzene (C) being obtained as the sole product (Fig. S5†). To further investigate the synergetic effect of the ternary oxides, H_2-pretreated binary oxide catalysts including $CuCeO_x$, $CuCoO_x$, and $CoCeO_x$ were prepared and the catalytic results indicated that ethylbenzene (C) was obtained in the presence of $CuCeO_x$ and $CuCoO_x$, and when using $CoCeO_x$ as the catalyst, only reduction of the carbonyl group can be achieved, affording 1-phenylethanol as the product. That is, none of them showed the ability to hydrogenate the benzene ring. In addition, selective hydrogenation was realized using catalysts obtained by pre-treating $Cu_1Co_5Ce_5O_y$ under hydrogen with different times. Then, the XPS spectra of the $CuCoO_x$ and $CuCeO_x$ were measured (Fig. S6†). It can be found that without the synergistic effect of CoO_x and CeO_x, the Cu species in $CuCoO_x$ and $CuCeO_x$ after H_2 pre-treatment all existed as Cu^{2+} and Cu^0, and controlled reduction to Cu^+ cannot be achieved. This was also proved by CODRIFTS as shown in Fig. S7.† Therefore, Cu^+ was the key factor in this work to achieve successful hydrogenation of the benzene ring. The generated $Cu_1Co_5Ce_5O_x$ catalysts exhibited distinct hydrogenation capabilities. As summarized in Fig. 4c, H_2-pretreatments for 6 h, 18 h, and 24 h lead to the formation of 96% ethyl benzene (C), 98% ethyl benzene (C), and 97% ethyl cyclohexane (D), respectively. Therefore, the H_2-pretreated ternary Cu–Co–Ce oxides show an excellent capability towards the hydrogenation of aromatic rings.

As previously reported, compared with Cu^0 and Cu^{2+}, Cu^+ has a higher hydrogenation activity considering its intrinsic ability to facilitate electron transfer through gaining or losing an electron.[25,30,31] Many studies have reported that Cu^0/Cu^+ leads to

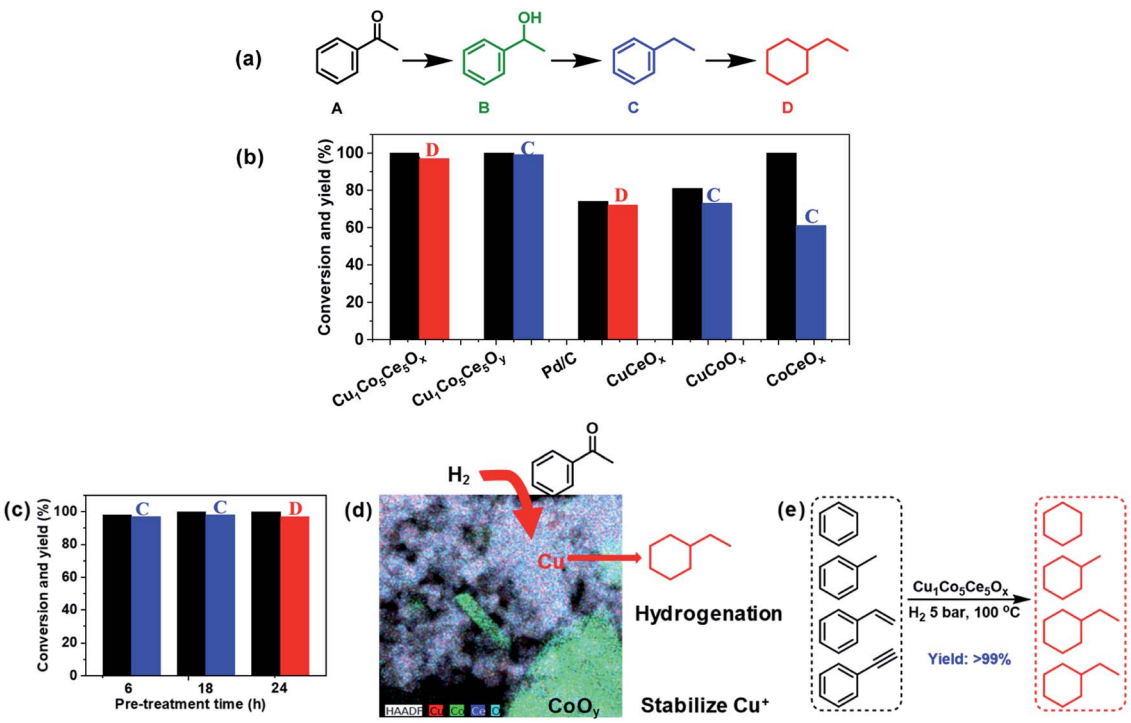

Fig. 4 (a) Catalytic hydrodeoxygenation of acetyl benzene. (b) Comparison of the catalytic activity using $Cu_1Co_5Ce_5O_x$, $Cu_1Co_5Ce_5O_y$, Pd/C, $CuOCeO_2$, CoO_yCeO_2, and $CuOCoO_y$ after H_2 pretreatment. (c) Catalytic hydrodeoxygenation of acetyl benzene over the $Cu_1Co_5Ce_5O_y$ catalyst with different pre-treatment times. (d) Synergistic effect of Cu_2O, CoO_y and CeO_2 in the CCC catalyst. (e) Hydrogenation of other aromatic compounds containing the benzene ring. All the reactions were performed under the following conditions: catalyst (100 mg), hexane (5 mL), substrate (1.25 mmol), reaction time (24 h), temperature (100 °C), H_2 (5 bar). Acetyl benzene was used as the substrate for the results in (a) and (b).

Open Access Article. Published on 22 May 2020. Downloaded on 2/9/2026 12:03:23 AM. This article is licensed under a Creative Commons Attribution-NonCommercial 3.0 Unported Licence.

an enhanced catalytic activity for hydrogenation, which is attributed to the activation of the ester groups by Cu^+ species.[30,33,34] However, it is difficult to isolate Cu^+ species for direct comparison, as it can rapidly convert to Cu^0 or Cu^{2+} during catalyst preparation and processing. Here we report a ternary oxide system $Cu_1Co_5Ce_5O_x$ where Cu^+ can be formed and stabilized through a simple pretreatment under H_2. As previously reported, the CoO_y in Cu catalyst not only enhances the metallic Cu dispersion and H_2 activation ability, but also modifies the chemical states of Cu to create suitable surface Cu^0/Cu^+ distributions due to strong electronic interactions at the Cu/CoO_x interface.[35] In our case, Cu is doped into the lattices of CoO_y and CeO_2 for $Cu_1Co_5Ce_5O_x$ and CoO_y exists as a promoter to stabilize Cu^+ under 5 bar H_2 and 100 °C through interfacial effects with CeO_2. This is further supported by the emergence of Cu^0 after the pretreatment of $CuCeO_x$ (Fig. S6 and S7†), indicating that Cu^{2+} will be reduced to Cu^0 without cobalt. The stabilized Cu^+ in $Cu_1Co_5Ce_5O_x$ exhibits an excellent catalytic performance for the hydrogenation of both benzene and C=O, while $CuCeO_x$, $CuCoO_x$, and $CoCeO_x$ exhibit limited conversion and selectivity of converting acetyl benzene to ethylcyclohexane. It was also reported that the defect-enriched CeO_2 constructed interfacial frustrated Lewis pairs ($Ce^{3+}\cdots O^{2-}$) that effectively activate the H_2 and CO_2 (ref. 38 and 39) and XPS results show that the H_2 pretreatment led to the formation of Ce^{3+} with oxygen vacancies on the surface. Chen *et al.*[51] also reported that the Cu^+ species directly bonded to the oxygen vacancy in CeO_2 exhibits a high activity for the water-gas shift reaction, where the Cu^+ site chemically adsorbs CO while the neighbouring O_v–Ce^{3+} site activates H_2O. Thus, CeO_2 functions as a hydrogen dissociation and transfer medium *via* the $Ce^{3+}\cdots O^{2-}$ frustrated Lewis pairs[54] and then the neighbouring Cu^+ hydrogenates the benzene as shown in Fig. 4d. In addition, benzene temperature programmed desorption (Ben–TPD) was performed to study the adsorption capacity of the benzene ring on $Cu_1Co_5Ce_5O_y$ and $Cu_1Co_5Ce_5O_x$ catalysts as shown in Fig. 3d. The two observed peaks at 100–200 and 250–450 °C are attributed to physical and chemical adsorption of benzene on the two oxide catalysts, respectively. Clearly, chemisorption of benzene on $Cu_1Co_5Ce_5O_y$ is enhanced after H_2 pretreatment as evidenced by the increase in desorption temperature from 250 °C to 420 °C, probably due to the strong interaction between benzene and a withdrawing Cu^+ from the oxygen ring.[55] Besides acetyl benzene, a series of benzene and benzene derivatives including benzene, phenylacetylene and methylbenzene are also fully hydrogenated to the corresponding alkanes using the $Cu_1Co_5Ce_5O_x$ catalyst under mild conditions (Fig. 4e), demonstrating the wide applicability of the ternary oxides for efficient benzene hydrogenation. In summary, a new type of Cu–Co–Ce ternary mixed oxide catalyst with remarkable hydrogenation activity of benzene is reported. Formation of Cu^+ during a simple pretreatment process is considered to be key to the activity promotion, while CoO_x functions as the Cu^+ stabilizer and CeO_2 facilitates the dissociation and transfer of hydrogen. Demonstration of Cu^+ in $Cu_1Co_5Ce_5O_x$ as the key component leading to extraordinary hydrogenation activity of substituted benzenes provides new insights into the design and modification of noble-metal-free catalysts for a wide scope of heterogeneous transformations. The resultant turnover number (TON) using $Cu_1Co_5Ce_5O_y$, $Cu_1Co_5Ce_5O_x$ and commercial 5 wt% Pd/C in this work was compared. The TON obtained in different catalytic systems was estimated based on the following equation: TON = mmol (ethylbenzene)/mmol (active site).[56,57] As a result, the TON of the $Cu_1Co_5Ce_5O_y$, $Cu_1Co_5Ce_5O_x$ and commercial 5 wt% Pd/C was calculated to be 0, 38.8 and 18.6. It was found that the $Cu_1Co_5Ce_5O_x$ obtained after H_2 pretreatment exhibited a TON value double that obtained using a Pd/C catalyst. The results of stability during five cycles of reuse as well as the XPS and XRD measurements are shown in Fig. S8–S10.† It was found that the Cu^+ remained in the 1^+ valence state after the hydrogenation (Fig. S8†). This is because the catalyst was pre-treated under the same conditions as the reaction conditions. Thus, during the reaction process within 24 h, the catalyst was stable and there should be no change of valence state during the catalytic recycling (Fig. S10†). The catalytic results revealed that the catalyst showed very good reusability for at least five cycles without any decrease in the catalytic activity, with >99% conversion of acetyl benzene and >95% yield of ethylcyclohexane being obtained in the fifth run. And the XRD results showed that the structure of the recycled catalyst was maintained well after catalyzing the hydrogenation reaction.

Conflicts of interest

There are no conflicts to declare.

Acknowledgements

HC, ZZY, KCJ, and SD were supported by the Division of Chemical Sciences, Geosciences, and Biosciences, Office of Basic Energy Sciences, U.S. Department of Energy. JF was supported by the National Natural Science Foundation of China (No. 21978259 and 21706228), the Zhejiang Provincial Natural Science Foundation of China (No. LR17B060002) and the Fundamental Research Funds for the Central Universities. The STEM characterization used resources of the Center for Functional Nanomaterials, which is a U.S. DOE Office of Science Facility, at Brookhaven National Laboratory under Contract No. DE-SC0012704.

Notes and references

1 R. A. Johnstone, A. H. Wilby and I. D. Entwistle, *Chem. Rev.*, 1985, **85**, 129–170.
2 F. Meemken and A. Baiker, *Chem. Rev.*, 2017, **117**, 11522–11569.
3 D. Wang and D. Astruc, *Chem. Rev.*, 2015, **115**, 6621–6686.
4 L. Zhang, M. Zhou, A. Wang and T. Zhang, *Chem. Rev.*, 2020, **120**, 683–733.
5 L. Alig, M. Fritz and S. Schneider, *Chem. Rev.*, 2018, **119**, 2681–2751.
6 W. Wang, S. Wang, X. Ma and J. Gong, *Chem. Soc. Rev.*, 2011, **40**, 3703–3727.

 This journal is © The Royal Society of Chemistry 2020

Open Access Article. Published on 22 May 2020. Downloaded on 2/9/2026 12:03:23 AM.
This article is licensed under a Creative Commons Attribution-NonCommercial 3.0 Unported Licence.

7 S. Miao, Z. Liu, B. Han, J. Huang, Z. Sun, J. Zhang and T. Jiang, *Angew. Chem. Int. Ed.*, 2006, **45**, 266–269.
8 C. P. Rader and H. A. Smith, *J. Am. Chem. Soc.*, 1962, **84**, 1443–1449.
9 L. Foppa and J. Dupont, *Chem. Soc. Rev.*, 2015, **44**, 1886–1897.
10 X. Kang, G. Luo, L. Luo, S. Hu, Y. Luo and Z. Hou, *J. Am. Chem. Soc.*, 2016, **138**, 11550–11559.
11 H. Liu, R. Fang, Z. Li and Y. Li, *Chem. Eng. Sci.*, 2015, **122**, 350–359.
12 C. Hubert, E. G. Bilé, A. Denicourt-Nowicki and A. Roucoux, *Green Chem.*, 2011, **13**, 1766–1771.
13 H. Liu, T. Jiang, B. Han, S. Liang and Y. Zhou, *Science*, 2009, **326**, 1250–1252.
14 P. Zhang, T. Wu, T. Jiang, W. Wang, H. Liu, H. Fan, Z. Zhang and B. Han, *Green Chem.*, 2013, **15**, 152–159.
15 K. M. Bratlie, H. Lee, K. Komvopoulos, P. Yang and G. A. Somorjai, *Nano Lett.*, 2007, **7**, 3097–3101.
16 C. Vangelis, A. Bouriazos, S. Sotiriou, M. Samorski, B. Gutsche and G. Papadogianakis, *J. Catal.*, 2010, **274**, 21–28.
17 P. Tomkins, E. Gebauer-Henke, W. Leitner and T. E. Müller, *ACS Catal.*, 2014, **5**, 203–209.
18 J.-F. Yuan, C.-Q. Luo, Q. Yu, A.-P. Jia, G.-S. Hu, J.-Q. Lu and M.-F. Luo, *Catal. Sci. Technol.*, 2016, **6**, 4294–4305.
19 X. Kang, H. Liu, M. Hou, X. Sun, H. Han, T. Jiang, Z. Zhang and B. Han, *Angew. Chem., Int. Ed.*, 2016, **55**, 1080–1084.
20 R. Molina and G. Poncelet, *J. Catal.*, 2001, **199**, 162–170.
21 L. Lu, Z. Rong, W. Du, S. Ma and S. Hu, *ChemCatChem*, 2009, **1**, 369–371.
22 Z. Zhang, Q. Yang, H. Chen, K. Chen, X. Lu, O. Pingkai, J. Fu and J. G. Chen, *Green Chem.*, 2017, **20**, 197–205.
23 Z. Zhang, S. Yao, C. Wang, M. Liu, F. Zhang, X. Hu, H. Chen, X. Gou, K. Chen, Y. Zhu, X. Lu, P. Ouyang and J. Fu, *J. Catal.*, 2019, **373**, 314–321.
24 B. An, J. Zhang, K. Cheng, P. Ji, C. Wang and W. Lin, *J. Am. Chem. Soc.*, 2017, **139**, 3834–3840.
25 J. Gong, H. Yue, Y. Zhao, S. Zhao, L. Zhao, J. Lv, S. Wang and X. Ma, *J. Am. Chem. Soc.*, 2012, **134**, 13922–13925.
26 Z.-Q. Wang, Z.-N. Xu, S.-Y. Peng, M.-J. Zhang, G. Lu, Q.-S. Chen, Y. Chen and G.-C. Guo, *ACS Catal.*, 2015, **5**, 4255–4259.
27 S. Kattel, P. J. Ramírez, J. G. Chen, J. A. Rodriguez and P. Liu, *Science*, 2017, **355**, 1296–1299.
28 R. Reske, H. Mistry, F. Behafarid, B. R. Cuenya and P. Strasser, *J. Am. Chem. Soc.*, 2014, **136**, 6978–6986.
29 S. Zhao, H. Yue, Y. Zhao, B. Wang, Y. Geng, J. Lv, S. Wang, J. Gong and X. Ma, *J. Catal.*, 2013, **297**, 142–150.
30 X. Chang, T. Wang, Z. J. Zhao, P. Yang, J. Greeley, R. Mu, G. Zhang, Z. Gong, Z. Luo, J. Chen, Y. Cui, G. A. Ozin and J. Gong, *Angew. Chem. Int. Ed.*, 2018, **57**, 15415–15419.
31 W. Chen, T. Song, J. Tian, P. Wu and X. Li, *Catal. Sci. Technol.*, 2019, **9**, 6749–6759.
32 C. Wen, A. Yin, Y. Cui, X. Yang, W.-L. Dai and K. Fan, *Appl. Catal., A*, 2013, **458**, 82–89.
33 Y. Wang, Y. Shen, Y. Zhao, J. Lv, S. Wang and X. Ma, *ACS Catal.*, 2015, **5**, 6200–6208.
34 S. Zhang, Y. Ma, H. Zhang, X. Zhou, X. Chen and Y. Qu, *Angew. Chem. Int. Ed.*, 2017, **56**, 8245–8249.
35 J. Wu, G. Gao, P. Sun, X. Long and F. Li, *ACS Catal.*, 2017, **7**, 7890–7901.
36 D. Teschner, J. Borsodi, A. Wootsch, Z. Révay, M. Hävecker, A. Knop-Gericke, S. D. Jackson and R. Schlögl, *Science*, 2008, **320**, 86–89.
37 T. Mitsudome, Y. Mikami, M. Matoba, T. Mizugaki, K. Jitsukawa and K. Kaneda, *Angew. Chem. Int. Ed.*, 2012, **51**, 136–139.
38 S. Zhang, Z. Xia, Y. Zou, F. Cao, Y. Liu, Y. Ma and Y. Qu, *J. Am. Chem. Soc.*, 2019, **141**, 11353–11357.
39 S. Zhang, Z. Q. Huang, Y. Ma, W. Gao, J. Li, F. Cao, L. Li, C. R. Chang and Y. Qu, *Nat. Commun.*, 2017, **8**, 15266.
40 A. J. Binder, T. J. Toops, R. R. Unocic, J. E. Parks and S. Dai, *Angew. Chem. Int. Ed.*, 2015, **54**, 13263–13267.
41 W. Xiao, S. Yang, P. Zhang, P. Li, P. Wu, M. Li, N. Chen, K. Jie, C. Huang, N. Zhang and S. Dai, *Chem. Mater.*, 2018, **30**, 2924–2929.
42 C. He, Y. Yu, L. Yue, N. Qiao, J. Li, Q. Shen, W. Yu, J. Chen and Z. Hao, *Appl. Catal., B*, 2014, **147**, 156–166.
43 Y. Tak and K. Yong, *J. Phys. Chem. C*, 2008, **112**, 74–79.
44 N. R. Radwan, M. Mokhtar and G. A. El-Shobaky, *Appl. Catal., A*, 2003, **241**, 77–90.
45 H. Yan, H. Qin, W. Liang, X. Jin, Y. Zhang, X. Feng, Y. Liu, X. Chen and C. Yang, *Catal. Sci. Technol.*, 2019, **9**, 4909–4919.
46 Y. Tanaka, R. Kikuchi, T. Takeguchi and K. Eguchi, *Appl. Catal., B*, 2005, **57**, 211–222.
47 S. Zhu, X. Gao, Y. Zhu, W. Fan, J. Wang and Y. Li, *Catal. Sci. Technol.*, 2015, **5**, 1169–1180.
48 C. Yang, Z. Miao, F. Zhang, L. Li, Y. Liu, A. Wang and T. Zhang, *Green Chem.*, 2018, **20**, 2142–2150.
49 L. Vivier and D. Duprez, *ChemSusChem*, 2010, **3**, 654–678.
50 D. Mullins, S. Overbury and D. Huntley, *Surf. Sci.*, 1998, **409**, 307–319.
51 A. Chen, X. Yu, Y. Zhou, S. Miao, Y. Li, S. Kuld, J. Sehested, J. Liu, T. Aoki and S. Hong, *Nat. Catal.*, 2019, **2**, 334.
52 H. Chen, Q. Wang, X. Zhang and L. Wang, *Appl. Catal., B*, 2015, **166–167**, 327–334.
53 H. Chen, Q. Wang, X. Zhang and L. Wang, *Ind. Eng. Chem. Res.*, 2014, **53**, 19916–19924.
54 M. García-Melchor and N. López, *J. Phys. Chem. C*, 2014, **118**, 10921–10926.
55 E. Kukulska-Zając, P. Kozyra and J. Datka, *Appl. Catal., A*, 2006, **307**, 46–50.
56 A. Dubey, L. Nencini, R. R. Fayzullin, C. Nervi and J. R. Khusnutdinova, *ACS Catal.*, 2017, **7**, 3864–3868.
57 X. Shao, X. Yang, J. Xu, S. Liu, S. Miao, X. Liu, X. Su, H. Duan, Y. Huang and T. Zhang, *Chem*, 2019, **5**, 693–705.